CONVECTIVE AND RADIATIVE HEAT TRANSFER DURING REENTRY AND ADVANCED TECHNIQUES FOR THEIR SIMULATION

by

Thomas N. Canning

INTRODUCTION

Experimental engineering research has been largely devoted to simulation, in the laboratory, of phenomena and systems which are difficult, for one reason or another, to reproduce in full-scale tests. The success of these efforts at simulation in guaranteeing the final system performance has been in direct proportion to the success in choosing the proper parameters to be matched and to the exactness of scaling laws derived for use in projecting to full-scale behavior. In the best of all possible worlds one could always make his tests at the design conditions using the complete system under consideration. One example will suffice to show why this generally cannot be done.

The Apollo command module will enter the earth's atmosphere at about 11 km/sec and will have on board three people, whose value has been enhanced by recent experiences. If all of the bits and pieces as well as the subsystems necessary for the mission have not been checked thoroughly in the laboratory, the chances of the complete system operating are nil.

One bit of this system which - thanks to hundreds of fairly cheap laboratory tests and scores of careful theoretical studies - assumes a lessening threat to success is the heat-protection system. It is to this narrow part of the vast complex of technologies that the present discussion of simulation is devoted. Since Brooks[1] has discussed the study of material response, the present paper is further restricted to evaluation of expected heat loads.

These heat loads are conveniently divided into two components which can usually be treated separately, convection and radiation from the gas within the shock layer to the vehicle surface.

CONVECTIVE HEATING

The stagnation-point convective heat load on blunt hypervelocity bodies has been treated extensively by many investigators, for example, Lees[2] and Fay and Riddell[3] in the speed range up to 10 km/sec. Lees has also related the heating elsewhere on simple bodies to that at the stagnation point. Starting with the former problem we see, in Figure 1, that the heating rate normalized with respect to the body size and pitot pressure is nearly a linear function of the driving potential, that is, the difference between stagnation and wall enthalpy. As the flight speed increases above about 9 km/sec, the temperatures become high enough that partial ionization occurs. The influence of ionization on convective heating has been argued widely: the consensus of those theoreticians who have used the transport properties predicted by Hansen[4] for hot air is that the influence is fairly small; the controversy is essentially settled by results of actual measurements of heating rates in two types

of modern laboratory equipment. Figure 2 shows the experimentally determined heating and indicates that there is, at least, fair agreement among the experimenters.

Most of the data shown in Figure 2 were obtained by use of shock tubes; the remainder were collected from aeroballistic tests. The shock tube consists of a tube containing a sample of test gas, say, air, and a driver filled with gas at high pressure (Fig. 3). When the diaphragm which separates the chambers is ruptured, a shock moves through the test gas simulating the detached bow shock of a flying body. Instruments may be placed around the test area to study the physical and chemical changes wrought by the shock compression. The pertinent setup for the study of convection requires small aerodynamic models to be mounted within the tube to simulate the hypervelocity flow field. Thin-film resistance gages or thicker calorimeter gages are deposited on the models so that the history of surface temperature, and hence heating rate, can be determined.[5, 6, 7]

The two most popular shock-tube configurations in use today are illustrated in Figure 4. The simplest form (in the upper sketch) uses the flow just behind the incident wave as the airstream. This part of the gas flow is very hot so that, even though its speed may be high, its Mach number is low and the aerodynamics of the test flow must be analyzed accordingly. This disadvantage is not serious when only the stagnation point heat transfer is being measured or when the details of the flow field are well known. The other configurations will be discussed later. Only a fraction of available convective-heating data (obtained in simple shock tubes) are shown in Figure 2. As with most rapidly developing experimental techniques, the data scatter unacceptably at the higher enthalpy, that is, velocity, levels. Most but not all of the apparent discrepancies are at least partially understood.

If the researchers using shock tubes had been content to use only the simplest designs, the description of the research done by them might be made more nearly complete; because these people have been inventive, the emphasis is necessarily put on descriptions of other shock-tube designs.

Variants on Simple Shock Tubes

The fact that the Mach number in the flow behind the incident wave is low, even when the wave speed is very high, has prompted investigators to employ simple expansion nozzles to cool the air adiabatically as well as increase its speed. Both of these effects are desirable, but the already short test times, a few milliseconds at best, are further eroded by starting and stopping transients. As the shock and its following gas sample starts into the expanding tube, the expansion and compression waves necessary to make the air adjust to the new flow geometry develop. Until the flow has become steady, test results are of doubtful value.

The net effect of this loss of testing time has been greatly reduced by introduction of the reflected-shock hypersonic-nozzle configuration in wide use today (see Fig. 4).

In this facility full advantage may be taken of the fact that upon reflection of the initial wave from the shock-tube end wall (the convergent part of the nozzle), the hot gas is brought to rest and heated further. This gas in the stagnation chamber advances slowly towards the nozzle and is used at less than one-tenth of the rate it would be used were there no constriction. The small nozzle throat also makes feasible the construction of moderate-sized hypersonic nozzles having very large expansion ratios

(greater than 1000) to accelerate the flow to high speed and low static temperatures (hence high Mach number).

The thermodynamic state in the test region is somewhat less perfectly understood than that in the stagnation chamber because of possible non-isentropic flow through the nozzle. This disadvantage is offset by the great gain in steady flow duration. The testing done in these reflected-shock-tube hypersonic tunnels may be made more representative of real flight because the Mach number, and hence inviscid flow phenomena, may be more adequately imitated than in the simple, straight tube. The importance of this simulation has been demonstrated in references 8 and 9, where it was shown that the strong bow wave of a blunt-nosed slender body, such as that shown in Figure 5, may seriously impair the stabilization afforded by flares and fins. This effect arises from severe changes in static and dynamic pressure distributions; the correspondence between pressure and heat load shown by Lees leads one to expect similar complications here. It is safe to say that if we are to simulate the heat-load distribution, we must simulate pressure distribution. The utility of the reflected-shock, hypersonic tunnel is well recognized for this reason.

A new entry to the field is the so-called expansion tube.[10] In this device the steady expansion through the nozzle of the shock-tube wind tunnel is replaced by an unsteady expansion into a nearly completely evacuated tube. The stream velocity capability is approximately double that of the nozzle-type facility. The steady flow duration just ahead of the unsteady expansion, on the other hand, is far shorter. Since the exploitation of this concept is just starting, it is difficult to predict its success. It is anticipated that simple extensions of shock-tube technology will make it very useful.

Ballistic Facilities

The course of imitation taken in shock-tube testing, that is providing a fast-moving hot or cold airstream, is a natural extension of older conventional wind-tunnel technology. A completely different approach has arisen from recent evolution of ballistic-range techniques. Development of guns capable of firing test bodies at speeds up to 10 km/sec provides us with the opportunity of observing actual flying bodies in the laboratory. By suitable adjustment in test parameters it is possible to simulate in varying degree most of the important governing phenomena. These hypervelocity projectors are called light-gas guns because they commonly use hot compressed hydrogen as a propellant. Differences in detail inevitably exist, but the schematic in Figure 6 shows the essentials of the best guns.

A small charge of gun powder is used to propel a heavy piston through the pump tube, thereby compressing the hydrogen it contained to peak pressures estimated to exceed 20,000 atm. As the pressure rises past about 1,000 atm, a thick steel diaphragm separating the pump tube from the launch tube ruptures and opens in four petals; and the hydrogen propels the model at accelerations exceeding a million g's to velocities exceeding 10 km/sec. The piston is arrested in the conical transition between the two tubes. These guns can launch well-designed models of remarkable complexity without damage, as will be discussed later.

The principal uses in defining the convective-heating environment expected in hypervelocity flight have been by detection of the onset of ablation of metal models as a measure of local maximum total heating rate, by calorimeter measurements of the total heat transferred to models which do and do not ablate, and by measurement of the surface-temperature histories

of the models with on-board thermocouple circuits.

These techniques have been described in references 11 and 12 but will be outlined herein for completeness. In the first method the many shadowgraph pictures taken of the model during its flight are studied to determine the time at which melting of the surface first commenced (see Fig. 7). This melting permits material to flow into the wake, where it can cast a shadow in the pictures. The analysis of the data consists of finding the theoretical prediction of heating rate which predicts the observed phenomena. This method has been checked directly against heat-transfer measurements in shock tubes and other facilities and found to be reliable. Subsequently, tests have been performed at flight speeds above 11 km/sec (Fig. 2).

At launch speeds below about 6 km/sec the small models used in these studies do not begin to melt, but simply absorb the heat. The second method method of measurement uses a calorimeter, into which the model drops, to measure this heat input. The apparatus used is shown in Figures 8 and 9. The model, after leaving the light-gas gun, flies along the ballistic range until it decelerates to low speed and is caught in the laminated paper-model catcher. It then drops into a calorimeter, where the heat increment is measured. By combining measurements made at a variety of muzzle velocities the variation of total heating with speed is deduced.

The third method of convective-heat-transfer measurement is the use of telemetered signals from the model to antennae along the flight path. Active FM telemetry has been developed for this work, but has not been usable in the speed range of interest because the acceleration loads are too great. A passive system has been developed using the principles

indicated in Figures 10 and 11. In this case a model containing a complete thermocouple circuit, including a four-turn coil, is fired at high speed. The surface junction is heated and the resulting emf produces a magnetic field. This dipole field, passing through the pickup coils, produces signals which can be analyzed to determine the temperature history of the surface and hence heating rate. This technique has been used to measure stagnation-point and afterbody-heating rates on blunt bodies at speeds up to 5.6 km/sec.

RADIATIVE HEATING

As mentioned earlier, the heating environment also includes radiative transport of energy from the hot shock layer to the surface. Since the consequences of radiation are proportionately more severe than convection, in terms of material removal from the heat shield, it is necessary that we measure this source fairly well for high-speed flight. The radiation is a consequence of excitation of internal degree of freedom of the gas molecules and atoms; if de-excitation occurs spontaneously, rather than by virtue of collisions with other particles, radiation is emitted. At high speeds this radiation becomes an important, perhaps, dominant, heat load on large bodies.

The emission and absorption spectra of thermally excited gases have been studied intensively in recent years. Several papers specializing in thermal radiation from air[13, 14, 15] agree acceptably in the speed range where radiative heating is small. These same discrepancies become unacceptable when considering flight at 15 km/sec. Figure 12 summarizes results from some of the experimental and theoretical work based on

shock-tube and ballistic tests. A simple application of these data to flight of a bluff body, 1 meter in radius, at 10 km/sec at 60 km altitude, shows an expected radiative heat load of about 200 watts/sq cm. This is probably not too serious, but the precipitous increases with increasing speed impels us to pin down the answers more precisely. The chief experimental tools for this work are shock tubes and ballistic ranges. This is not to say that no other facility can supply a hot-gas sample for study; the chief justification advanced here is that the thermodynamic state of the gas in these two types of test is quite precisely known and relatable to full-scale flight; since the mode of heat addition to the gas is identical to that in flight, we have even more confidence. For these tests the shock tube was historically first and in some aspects the more versatile facility.

Returning to the shock tube, Figure 13, we see that, as the incident wave passes through the test section, it usually duplicates the normal shock ahead of a hypervelocity blunt body. The absolute spectral emission from the gas behind the wave front can be determined from groups of radiometers placed to look through the test volume. It has been found possible to survey with sufficient spatial resolution to unravel some of the chemical changes within the reaction zone behind the wave front. As these net reactions cease, on reaching equilibrium, the radiometer measurements yield the type of data on which Figure 12 is based. The reaction zone itself has attracted much interest as well because the higher-than-equilibrium temperatures result in radiation in excess of that which would have been emitted had equilibrium been achieved instantaneously.

The chief advantages of the shock tube lie in the near-perfect duplication of the essentially one-dimensional flow along the stagnation

streamline near the shock. Only at very low air densities do the tube walls interfere directly with the flow near the middle of the tube. On the other hand, all measurements of radiation are distorted by emission and absorption in the turbulent, nonuniform contaminated shock-tube boundary layer. It has proven very difficult to keep contamination at acceptable levels in many studies.

Much of the fundamental research on absolute emissive power of particular radiating species and the reaction rates in the flow just behind wave fronts has been done with shock tubes. Recently precise techniques have been devised for these studies in ballistic ranges. Radiation from complete three-dimensional flow fields is also measurable in these tests.

Essentially the hypervelocity ballistic test gives us a small object of known shape flying at known speed through a gas of selected properties. Within quite broad limits it is possible to simulate the physical, chemical, and thermodynamic properties of flows about full-scale vehicles.[16] The thermal radiation from these flows has been studied for several years at Ames Research Center. In these studies the absolute spectral emitted power is measured with radiometers mounted near the flight path of the model. The bandpasses of these devices are made narrow enough to make meaningful engineering measurements of heating rates but too wide to identify radiating species. An example of such data for flight at ballistic-missile speeds, taken from reference 17, is shown in Figure 14. The general verification of the predictions at short wavelengths is clear; the dependence of the infrared on model material is seen to be strong. This latter point is a whole field of study in itself and beyond the scope of this paper. The implications in the fields of radiative transport may be seen.

These measurements were made with assorted photomultiplier-filter combinations and are used to deduce the radiation per unit volume at the gas-cap stagnation conditions. These figures may then be applied point by point within the calculated shock layers of the full-scale body to estimate complete radiative heat loads.

Recently, as implied above, Reis has used the hot-stagnation-region gas on ballistic models as a radiation source and unusual measuring techniques to obtain the absolute band-system strengths of several molecular species.[18] The spectral resolution is sufficient in these tests to make accurate independent measurements of the transition probabilities, one of the fundamental properties necessary for rigorous prediction of absolute spectral emissive power at conditions different from those of the particular test.

It has proven to be possible to calculate theoretically the spectral distribution of relative intensity of remarkably complex band systems of molecular radiators. Recourse must be had to experiment if the absolute strengths are to be known. In practice the factor necessary to achieve agreement between theory and experiment is found. This factor may take the form of a transition probability or f-number.

The required spectra were obtained photoelectrically by means of a time-of-flight scanning spectrometer. This device is shown schematically in Figure 15. As the model flies by in the focal plane of the collecting mirror, the luminous gas cap acts as a moving entrance slit, sweeping out the spectrum of the shock-heated gas on the exit slit. (That the gas cap is the only source of radiation in the flow field and is indeed slit-like in form is shown in a typical image-converter photograph of a plastic model, Fig. 16.) The energy passing through the exit slit of the scanning

spectrometer is divided; 95 percent passes through a splitter plate and on to the cathode of an RCA 1P28 multiplier phototube. The output of this multiplier phototube is recorded on an oscilloscope and yields a continuously recorded spectrum over a wavelength range dictated mainly by the geometry of the system. For the tests reported in reference 18, the wavelength range was as a rule from 0.290 to 0.430μ. Figure 17 shows a typical oscillogram. The remaining 5 percent of the energy passes through a narrow-band interference filter (100 Å wide between the 50-percent response points) and onto a Dumont 6935 multiplier phototube. The output of this phototube is displayed on an oscilloscope which has been triggered so as to start sweeping simulataneously with the oscilloscope which records the spectrum. The auxiliary oscillogram thus allows a specific wavelength to be transposed to the oscillogram displaying the spectrum. Such wavelength transposition was found to be repeatable from shot to shot to $\pm$10 Å.

The time-of-flight scanning spectrometer was constructed by modifying a Farrand uv-vis f/3.5 grating monochromator. A large opening was cut in the monochromator housing in the region of the intended entrance slit and the standard collecting mirror was replaced by a spherical mirror which focused at the center of the test chamber. Further, the new collecting mirror was masked down to a rectangular slot to improve depth of field and to insure uniform illumination of the grating. The rise time of the complete system was 25 nanoseconds and was dictated by the oscilloscope.

Another instrument was devised in order to measure the spatial distribution of radiation over the faces of bluff models. These measurements were needed in order to substantiate calculations used in analyzing the above test results and also to describe more completely the real distribution.

The instrument in point required that a near head-on view of the model be imaged on a plate having tiny orifices opening onto a phototube (Fig. 18). The system effectively registers any light radiated from area sources along the optical axis. As the model flies by the optical axis, a scan of the shock layer occurs. Auxiliary equipment is used to determine where on the model the scan occurred. In this manner the actual distribution of radiative heat load can be measured. More recently head-on photographs (Fig. 19) have been taken successfully using image-converter and Kerr-cell-shutter cameras.

These photographs have been analyzed, using step-wedge filters for film calibration and microdensitometers for exposure measurements, to yield similar heat-load distributions. The agreement between the two systems is good. The advantage of the dissector is that it involves fewer experimental steps; the advantage of the photographic system is that is permits complete determination of the distribution rather than a few scans.

VELOCITY AUGMENTATION

Since tests at speeds above 7 or 8 km/sec are difficult in purely ballistic facilities, we have superposed a countercurrent airstream which can move as fast as 5 km/sec. This airstream is in a reflected-shock, hypersonic-wind-tunnel test section and the models are fired upstream (Fig. 20). Some data have been obtained in this manner at flight speeds above 13 km/sec.[19] The most reliable of these data, where the flow fields were known to be in equilibrium, extend above 12 km/sec (Fig. 12).

The chief advantages of this test facility lie in excellent simulation

of velocity, Mach number, Reynolds number, complete flow configuration, and degree of equilibration of all binary-scaled chemical and physical changes.

In still-air tests, it has proven possible to reduce contamination to negligible levels; also no stream boundary layer is present to distort the results. In air-on tests it appears simple to reduce contamination to acceptable levels. The drawbacks are that data extraction is not simple; much effort is required to advance the instruments and test techniques. The duration of observations is typically about a microsecond and the attitude and condition of the model must be accurately registered because it cannot be predicted. The thermodynamic simulation of the flow along streamlines can be quite nicely duplicated, but it has as yet been impractical to study individual stream tubes as has effectively been done in shock-tube flows.

CONCLUDING REMARKS

The use of shock tubes, ballistic ranges, and combinations thereof in simulation of convective and radiative heat loads has been described. The complementary nature and the highly independent techniques used in these facilities lend great strength to the research results where they agree. The shortcomings of these facilities are such that, if possible, both should be applied to important problems. When all-out performance is required, the combination of the two can clearly provide advantages. That these advantages are becoming more widely recognized is demonstrated by the construction of new facilities at Arnold Engineering Development

Center and Boeing Company, Seattle, similar to those in service at Ames Research Center since the late 1950's.

REFERENCES

1. Brooks' paper presented at same conference.

2. Lees, L.: Laminar Heat Transfer Over Blunt-Nosed Bodies at Hypersonic Flight Speeds. Jet Propulsion, vol. 26, no. 4, April 1956, pp. 259-269, 274.

3. Fay, J. A., and Riddell, F. R.: Theory of Stagnation Point Heat Transfer in Dissociated Air. Jour. Aero. Sci., vol. 25, no. 2, Feb. 1958, pp. 73-85, 121.

4. Hansen, C. Frederick: Approximations for the Thermodynamic and Transport Properties of High-Temperature Air. NASA TR R-50, 1959.

5. Rose, P. H., and Stark, W. I.: Stagnation Point Heat-Transfer Measurements in Dissociated Air. Jour. Aero. Sci., vol 25, no. 2, Feb. 1958, pp. 86-97.

6. Hoshizaki, H.: Heat Transfer in Planetary Atmospheres at Super-Satellite Speeds. ARS Journal, vol. 32, no. 10, Oct. 1962, pp. 1544-51.

7. Warren, W. R., Rogers, D. A., and Harris, C. J.: The Development of and Electrically Heated, Shock Driven Test Facility. Second Symposium on Hypervelocity Techniques, Denver, 1962.

8. Seiff, Alvin: Secondary Flow Fields Embedded in Hypersonic Shock Layers. NASA TN D-1304, 1962.

9. Terry, James E., and James, Carlton S.: A Parametric Study of Hypersonic Flow Fields About Blunt-Nosed Cylinders at Zero Angle of Attack. NASA TN D-2342, 1964.

10. Trimpi, R. L.: A Preliminary Theoretical Study of the Expansion Tube, A New Device for Producing High Enthalpy Short-Duration Hypersonic Gas Flows. NASA TR R-133, 1962.

11. Compton, Dale L., and Chapman, Gary T.: Two New Free-Flight Methods for Obtaining Convective-Heat-Transfer Data. Paper for AIAA Aerodynamic Testing Conference, March 9-10, 1964.

12. Yee, Layton, Bailey, Harry E., and Woodward, Henry T.: Ballistic Range Measurements of Stagnation-Point Heat Transfer in Air and in Carbon Dioxide at Velocities up to 18,000 Feet Per Second. NASA TN D-777, 1961.

13. Meyerott, R. E., Sokoloff, J., and Nicholls, R. W.: Absorption Coefficients of Air. LMSD 288052, Lockheed Aircraft Corp., 1959.

14. Kivel, B., and Bailey, K.: Tables of Radiation From High Temperature Air. Res. Rep. 21, AVCO-Everett Research Lab., 1957.

15. Breene, R. G., Nardone, Maria, Riethof, T. R., and Zeldin, Saydean: Radiance of Species in High Temperature Air. General Electric Space Sciences Lab., July 1962.

16. Gibson, W. E., and Marrone, P. V.: Nonequilibrium Scaling Criterion for Inviscid Hypersonic Airflows. QM-1626-A-8, Cornell Aero. Lab., 1962.

17. Page, William A., and Arnold, James O.: Shock-Layer Radiation of Blunt Bodies at Reentry Velocities. NASA TR R-193, 1964.

18. Reis, Victor H.: Oscillator Strength for the N_2 Second Positive and N_2^+ First Negative Systems From Observations of Shock Layers About Hypersonic Projectiles. Jour. of Quant. Spectrosc. and Radiat. Transfer, vol. 4, no. 6, 1964, p. 783.

19. Canning, Thomas N., and Page, William A.: Measurements of Radiation From the Flow Fields of Bodies Flying at Speeds Up to 13.4 Kilometers Per Second. Presented at the AGARD meeting, Brussels, Belgium, April 1962.

Figure 1. Theoretical laminar convective heating at stagnation point of hypervelocity spheres.

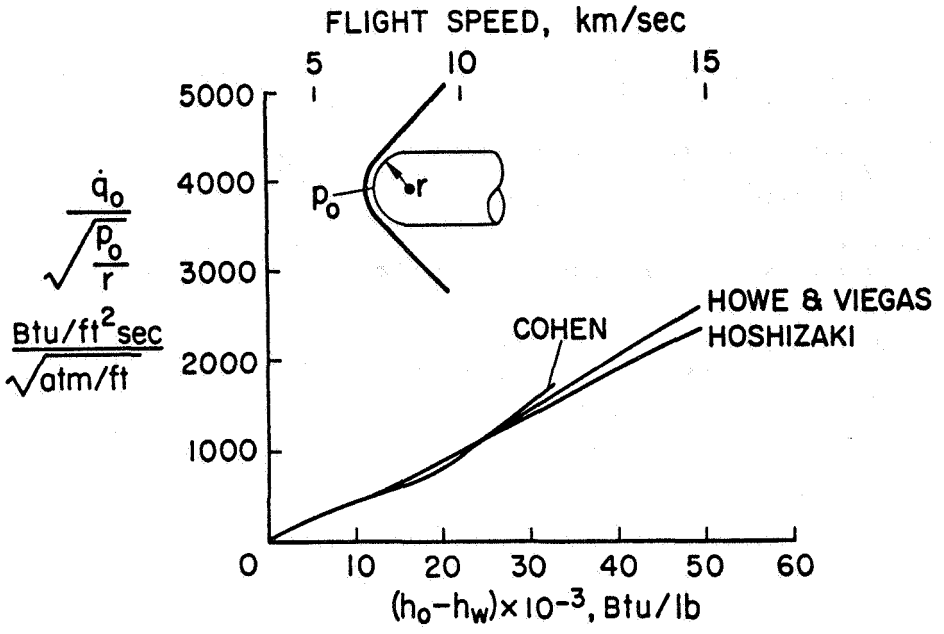

Figure 2. Experimental laminar convective heating at stagnation point of hypervelocity spheres.

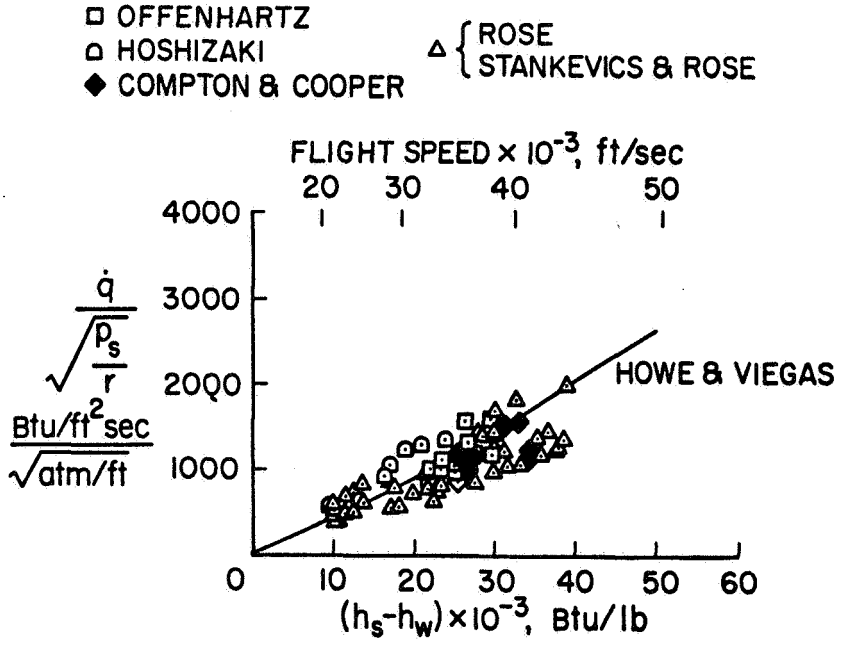

Figure 3. Simple shock tube.

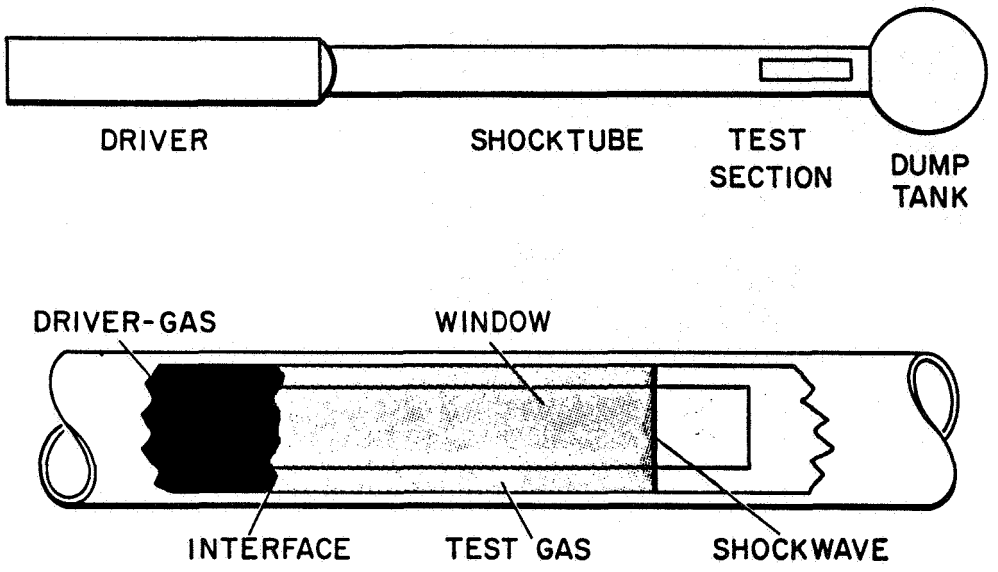

Figure 4. Popular modifications of simple shock tube.

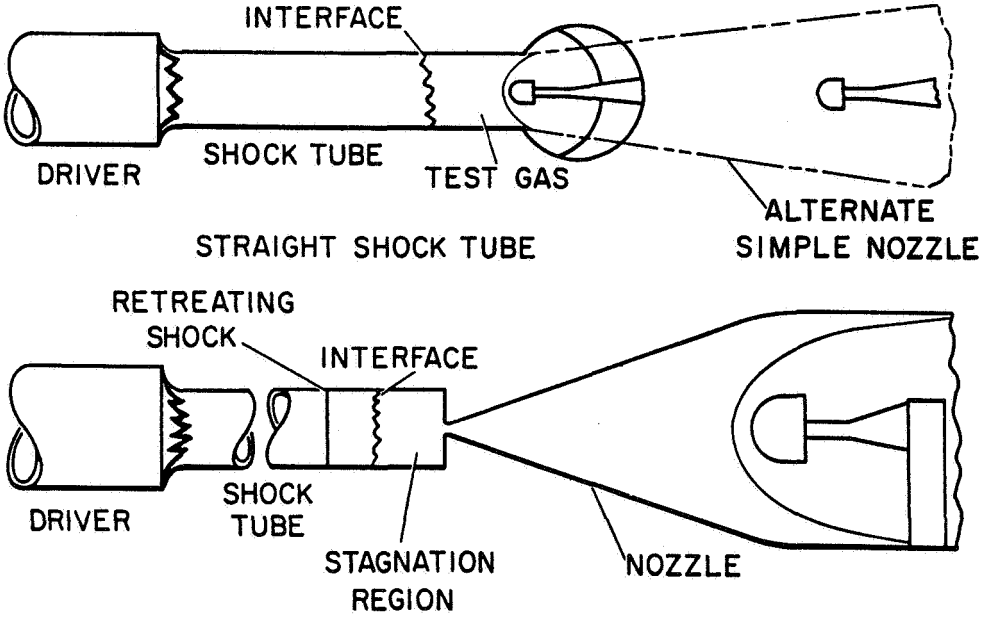

Figure 5. Shadowgraph of blunt-nosed cylinder showing embedded supersonic flow in hypersonic flow field.

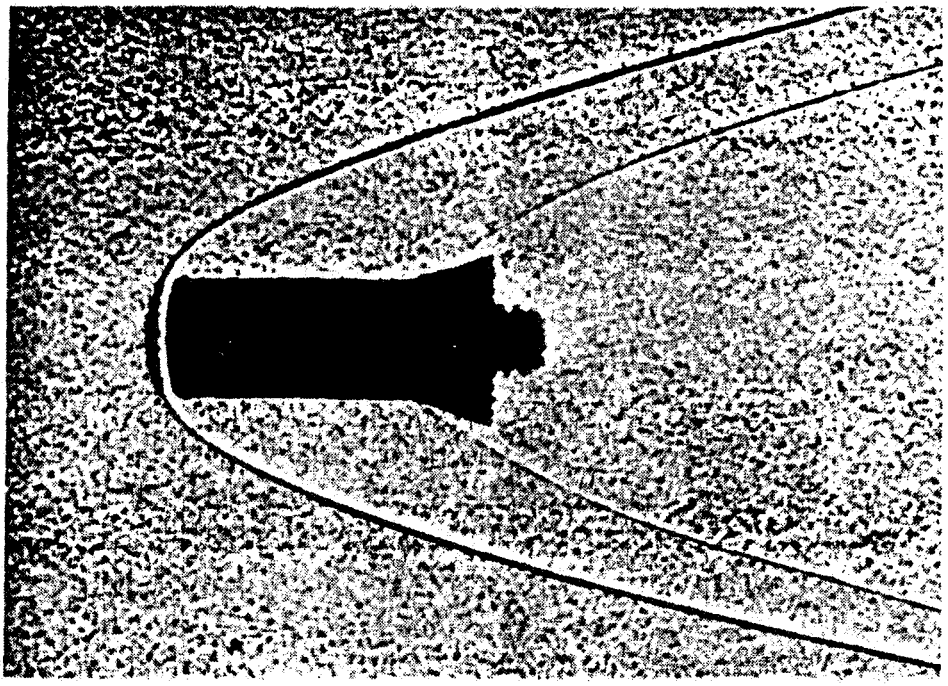

Figure 6. Deformable piston light-gas gun.

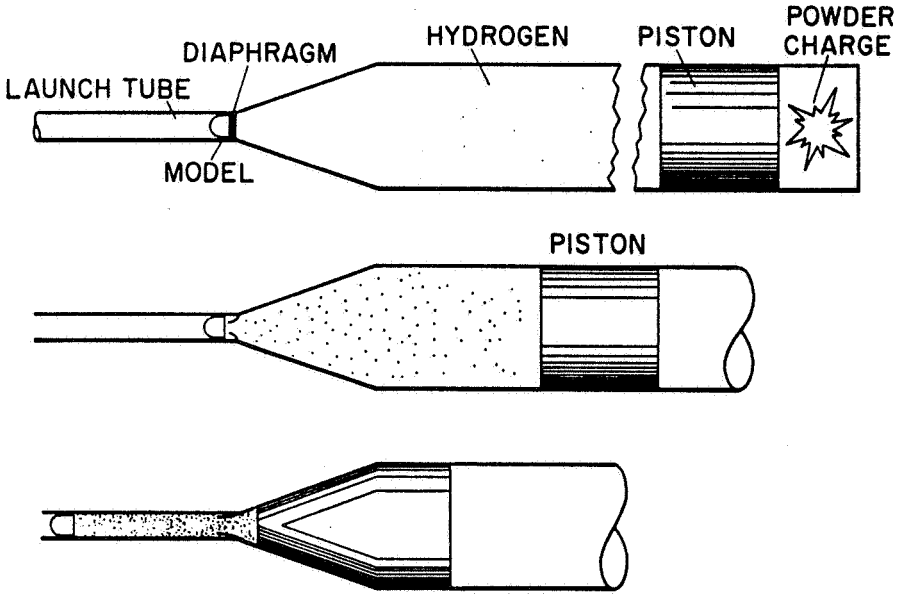

Figure 7. Shadowgraph sequence showing onset of ablation.

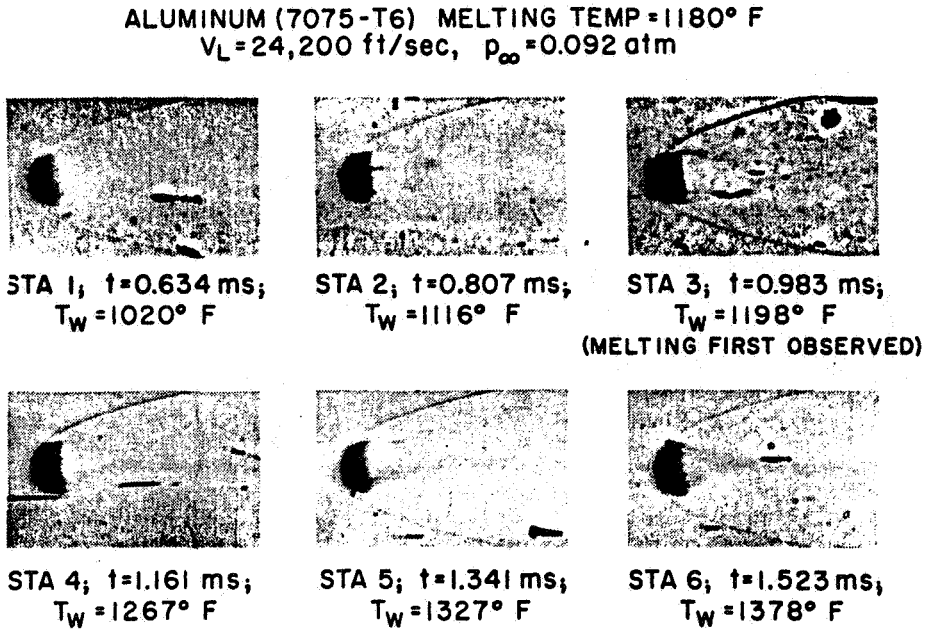

Figure 8. Ballistic range arrangement for calorimetry flights.

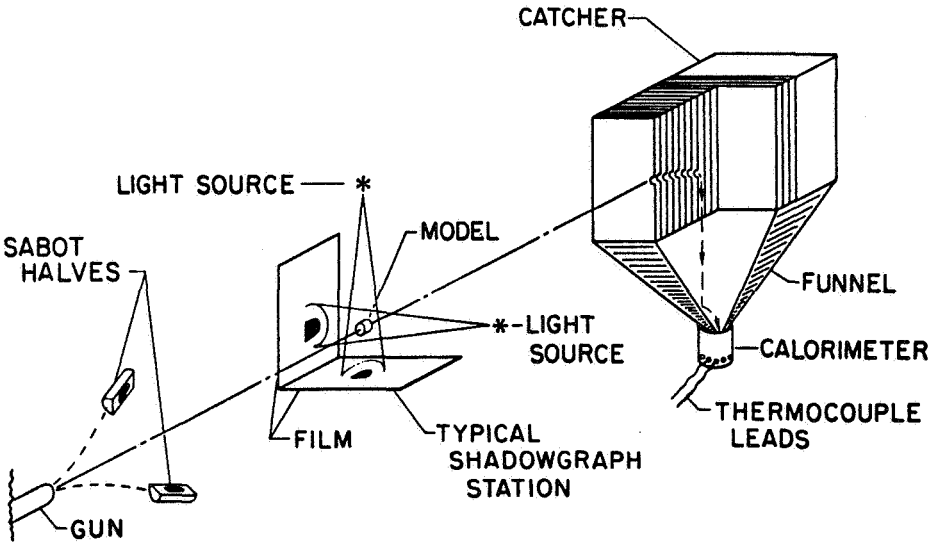

Figure 9. Calorimeter section.

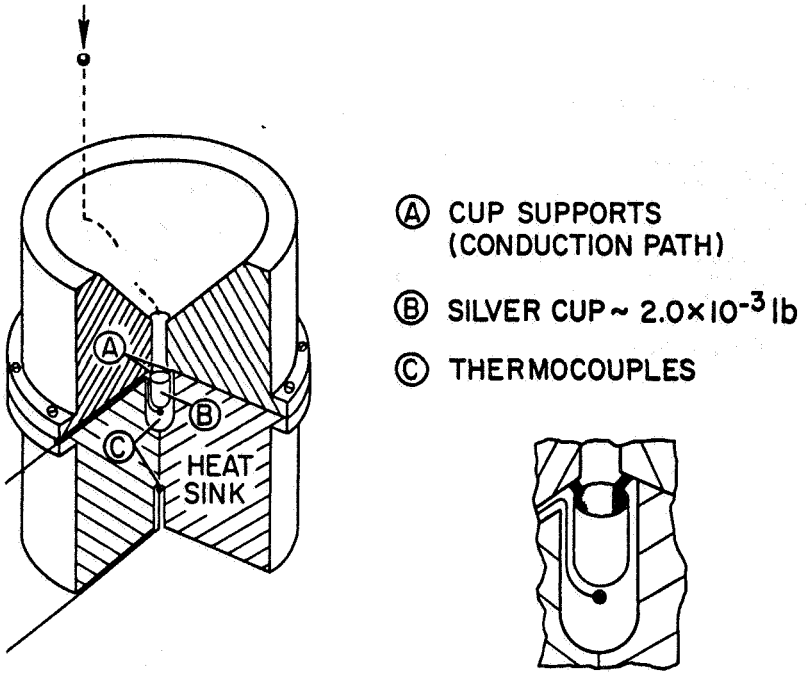

Figure 10. Thermocouple model for stagnation-point heating tests.

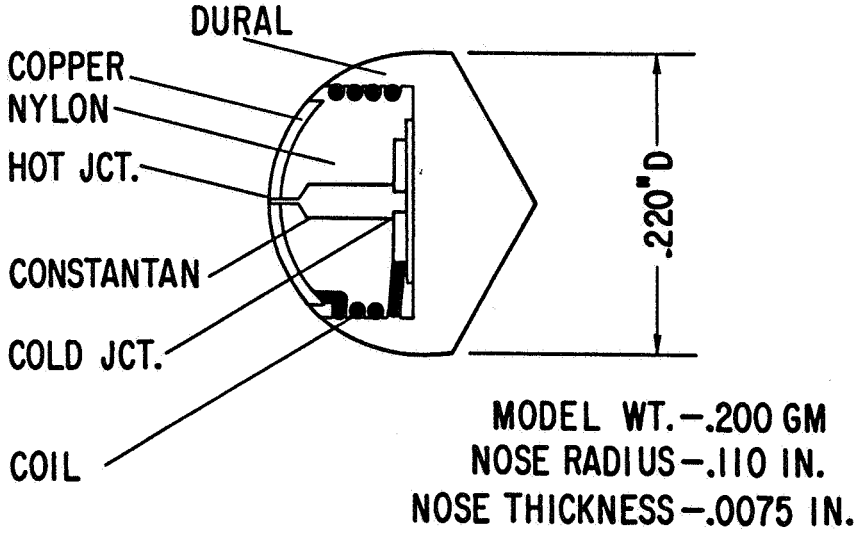

Figure 11. Ballistic range arrangement and antenna for thermocouple model flights.

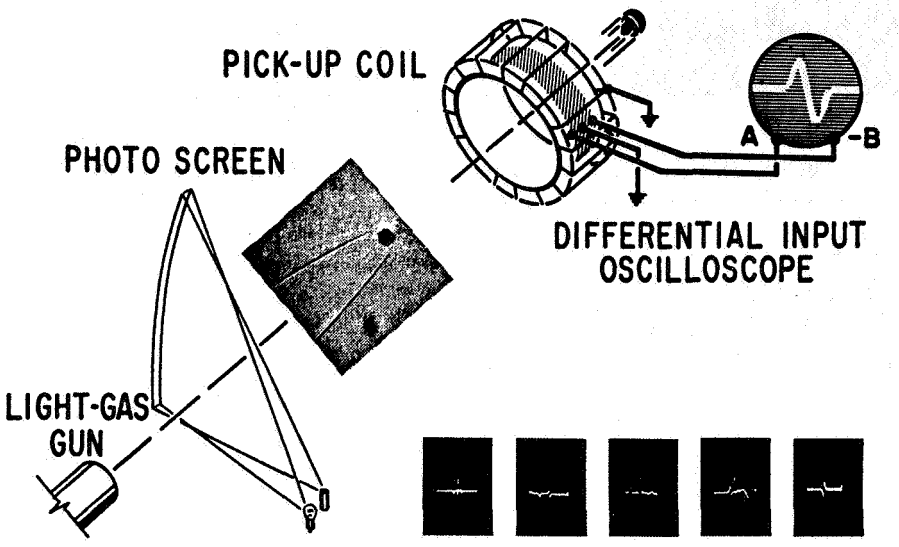

Figure 12., Variation with velocity of emissive power of air behind normal shock waves.

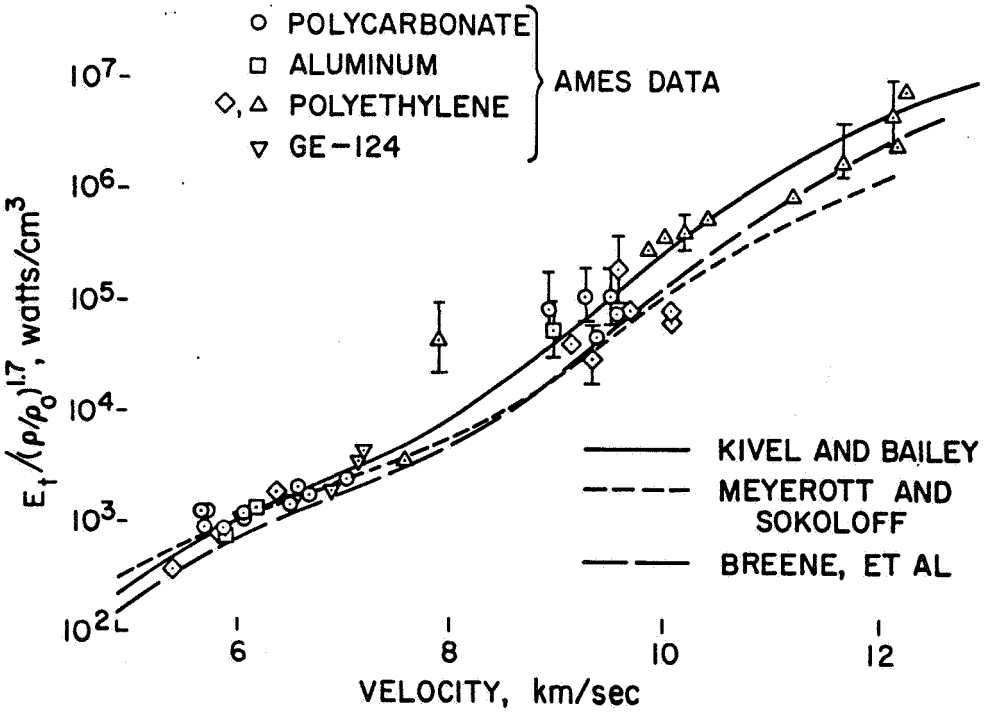

Figure 13. Nonequilibrium zone air radiation.

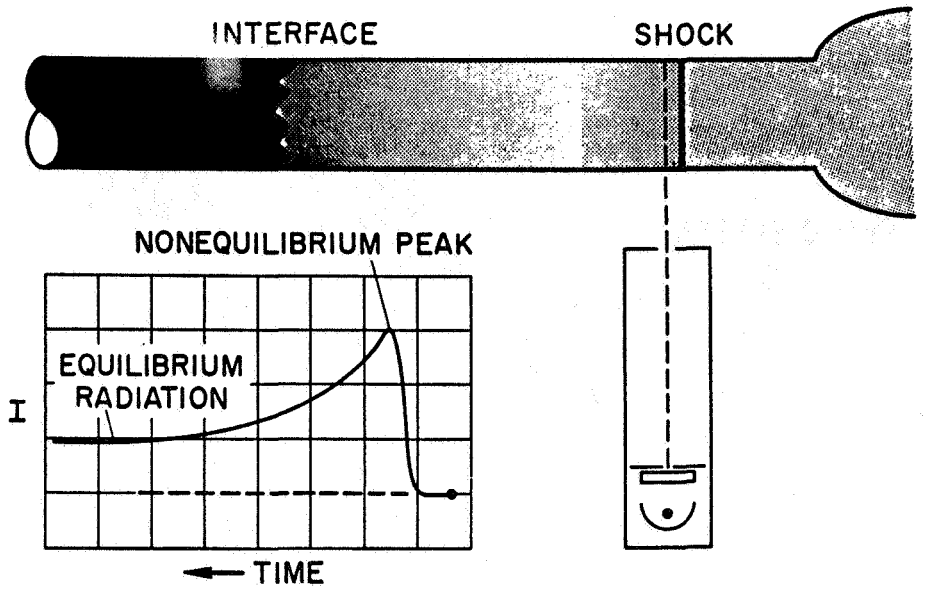

Figure 14. Absolute spectral emission from complete flow fields of bodies made of several materials.

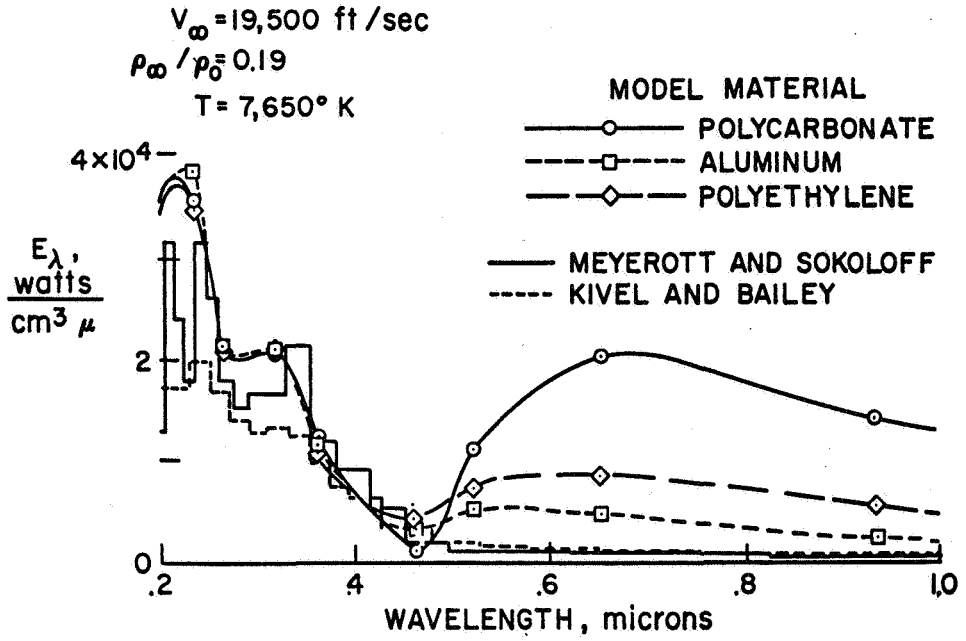

Figure 15. Time-of-flight scanning spectrometer.

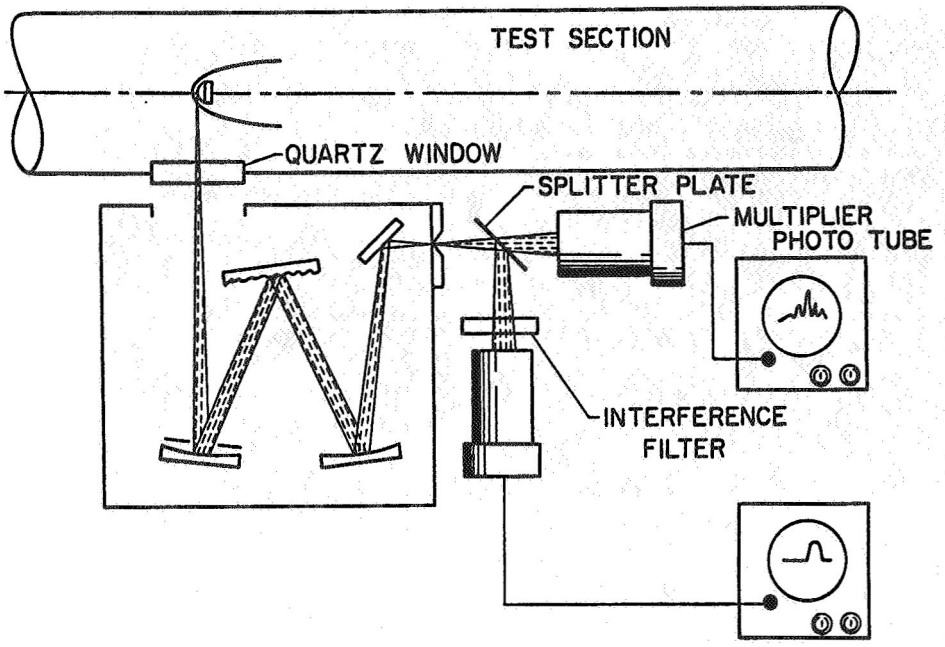

Figure 16. Image-converter photograph of polyformaldehyde model in flight at 5.5 km/sec; p_∞ = 60 mm Hg.

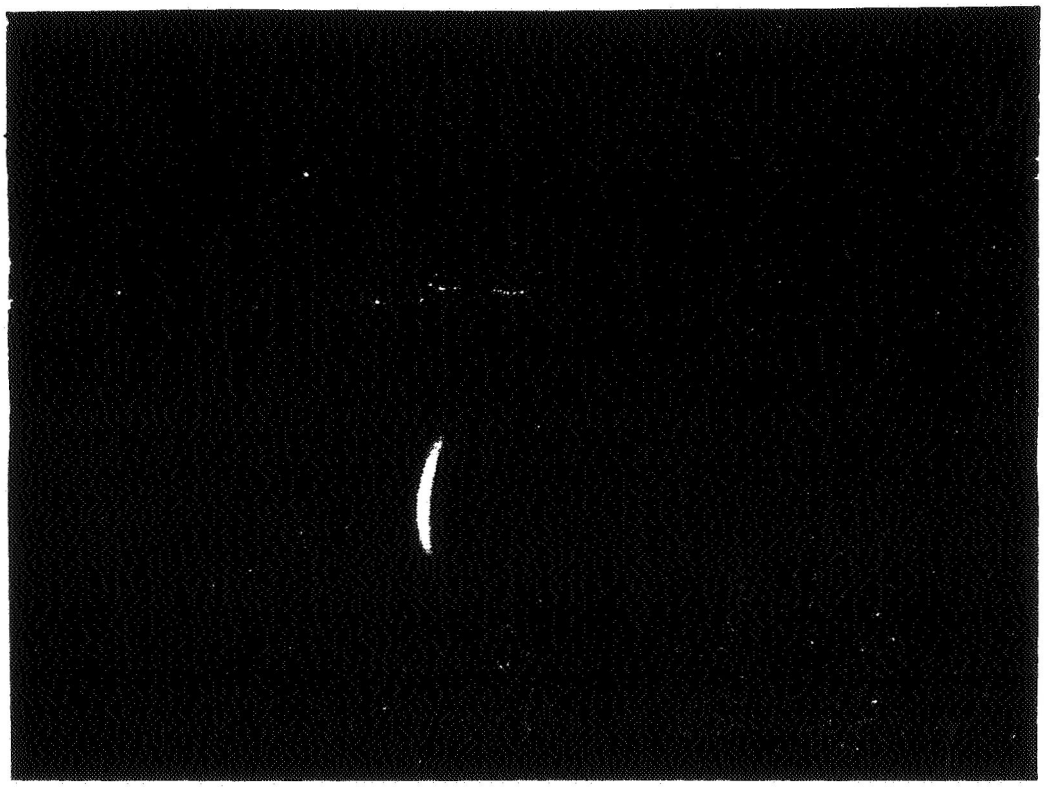

Figure 17. Oscillogram of near ultraviolet spectrum from time-of-flight scanning spectrometer.

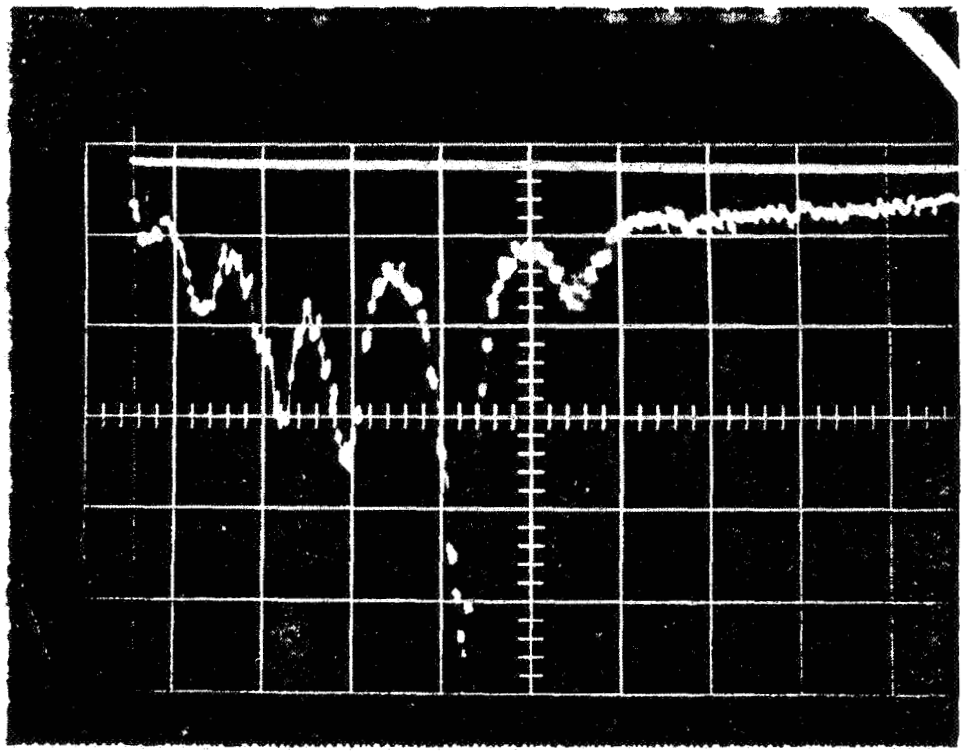

Figure 18. Image dissector scheme.

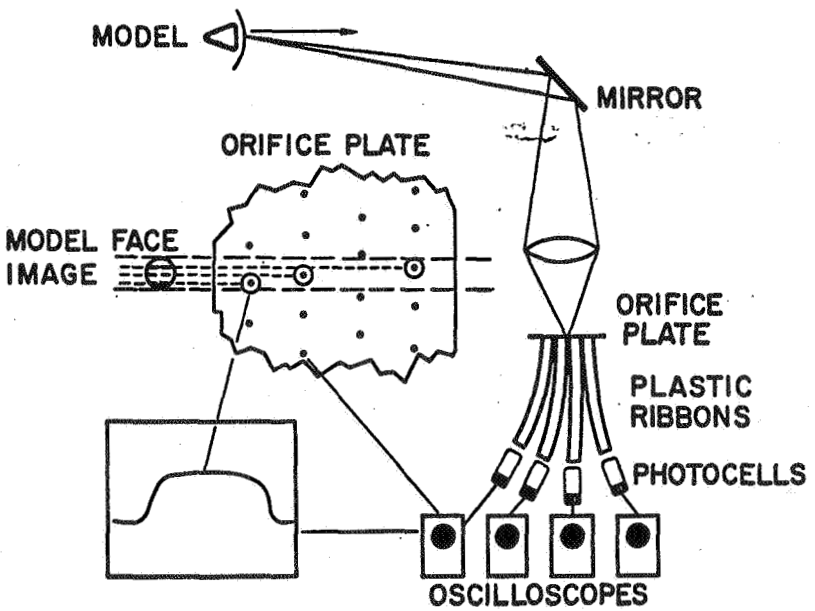

Figure 19. "Head-on" photograph of polycarbonate model flying through air at 6 km/sec; p_∞ = 60 mm Hg.

Figure 20. Schematic of counterflow facility.